International Journal of Remote Sensing
Vol. 29, No. 4, 20 February 2008, 1093–1107

Taylor & Francis
Taylor & Francis Group

Trajectory analysis of land cover change in arid environment of China

Q. ZHOU*†, B. LI‡ and A. KURBAN§

†Department of Geography, Hong Kong Baptist University, Hong Kong Kowloon Tong, Kowloon, Hong Kong

‡State Key Laboratory of Environment and Resources Information System Institute of Geographical Sciences and Resources Research, Chinese Academy of Sciences, Beijing, 100101, P.R. China

§Xinjiang Institute of Ecology and Geography, Chinese Academy of Sciences, 40-3 South Beijing Road, Urumqi, Xinjiang 830011, China

(*Received 8 May 2006; in final form 7 March 2007*)

Remotely sensed data have been utilized for environmental change study over the past 30 years. Large collections of remote sensing imagery have made it possible for spatio-temporal analyses of the environment and the impact of human activities. This research attempts to develop both conceptual framework and methodological implementation for land cover change detection based on medium and high spatial resolution imagery and temporal trajectory analysis. Multi-temporal and multi-scale remotely sensed data have been integrated from various sources with a monitoring time frame of 30 years, including historical and state-of-the-art high-resolution satellite imagery. Based on this, spatio-temporal patterns of environmental change, which is largely represented by changes in land cover (e.g., vegetation and water), were analysed for the given timeframe. Multi-scale and multi-temporal remotely sensed data, including Landsat MSS, TM, ETM and SPOT HRV, were used to detect changes in land cover in the past 30 years in Tarim River, Xinjiang, China. The study shows that by using the auto-classification approach an overall accuracy of 85–90% with a Kappa coefficient of 0.66–0.78 was achieved for the classification of individual images. The temporal trajectory of land-use change was established and its spatial pattern was analysed to gain a better understanding of the human impact on the fragile ecosystem of China's arid environment.

1. Introduction

Land cover change is one of the most sensitive indicators that echo the interactions between human activities and natural environment. In arid environments, where fragile ecosystems are dominant, the land cover change often reflects the most significant impact on the environment due to excessive human activities.

Remotely sensed data have been the most important data source for environment change study in the past 30 years and large collections of remote sensing imagery have made it possible to analyse spatio-temporal patterns of environmental elements and the impact of human activities. Research has been widely reported on methodology of remote sensing change detection and monitoring (e.g. Singh 1989, Lu *et al.* 2004).

*Corresponding author. Email: qiming@hkbu.edu.hk

International Journal of Remote Sensing
ISSN 0143-1161 print/ISSN 1366-5901 online
http://www.tandf.co.uk/journals
DOI: 10.1080/01431160701355256

Change detection approaches can be characterized into two broad groups, namely, bi-temporal change detection and temporal trajectory analysis (Coppin *et al.* 2004). The former measures land cover changes based on a 'two-epoch' timescale, i.e. the comparison between two dates. Even if land cover information is sometimes acquired for more than two epochs, the changes are still measured on the basis of pairs of dates. The latter analyses the changes based on a 'continuous' timescale, i.e. the focus of the analysis is not only on what has changed between dates, but also on the progress of the change over the period. At present, most change detection methods belong to the bi-temporal change detection approach including, for example, image differencing (e.g. Maktav and Erbek 2005), vegetation index differencing (Muttitanon and Tripathi 2005), change vector analysis (CVA) (e.g. Lunetta *et al.* 2004), principal component analysis (PCA) (e.g. Liu *et al.* 2004), post-classification comparison (Dewidar 2004), multi-temporal composite and classification (e.g. Zhao *et al.* 2004), and artificial neural network (ANN) (e.g. Liu and Lathrop Jr 2002).

In general the aim of bi-temporal change detection is to obtain details of 'change/no change' or 'from–to' information in between the detection dates. These methods are typically based on medium- and high-resolution remotely sensed images (e.g. Landsat TM, ETM, SPOT, IRS and AVIRIS), as its applications often require more accurate measurements on, for example, the area ratio changes (Harris 2003, Weber *et al.* 2005), the conversion matrix of land cover change (Zhao *et al.* 2004, Muttitanon and Tripathi 2005) and the spatial pattern changes characterized by land cover metrics changes (Narumalani *et al.* 2003, McConnell *et al.* 2004).

The temporal trajectory analysis is to discover the trend of the land cover change by constructing the 'curves' or 'profiles' of multi-temporal data. In contrast to bi-temporal change detection, the temporal trajectory analysis is mostly based on low spatial resolution images such as AVHRR and MODIS, which have a high temporal resolution. The trade-off of using these images, however, is the loss of spatial details that makes auto-classification very difficult with low accuracy, so that the temporal trajectory analysis is commonly restricted to, for example, vegetation dynamics in large areas (Lambin and Ehrlich 1997, Myneni *et al.* 1997, Kawabata *et al.* 2001, Dessay *et al.* 2004, Herrmann *et al.* 2005, Olsson *et al.* 2005), or change trajectories of individual land cover classes (Mertens and Lambin 2000, Petit *et al.* 2001, Crews-Meyer 2001, Southworth *et al.* 2002, Liu and Zhou 2005). Quantitative parameters such as normalized difference vegetation index (NDVI) or area of given land cover class are often used as the dependent variables for the establishment of change trajectories.

To study human impact on the natural environment, it is often required to recover the history of land cover change and relate the spatio-temporal pattern of such change to other environmental and human factors, rather than merely relying on the change of areas or indices. With the accumulation of remotely sensed images over the past 30 years, it is now possible to analyse the categorical changes of land cover types using higher resolution imagery. Attempts have been made and reported on the applications of bi-temporal change detection methods to multiple epochs (Masek *et al.* 2000, Herold *et al.* 2003, Liu and Zhou 2004, 2005, Lunetta *et al.* 2004, Tang *et al.* 2005). However, further research is needed to develop a methodology that can integrate methods of above bi-temporal change detection and temporal trajectory analysis so that the paths of land cover change for every location in an area can be traced.

This study seeks an efficient and practical methodology to integrate multi-temporal and multi-scale remotely sensed data from various sources with a monitoring timeframe of 30 years, including historical and state-of-the-art high-resolution satellite imagery. Based on this, the spatio-temporal pattern of environmental change, which is largely represented by the land cover (e.g. vegetation and water) change, has been analysed for the given timeframe. The history of land cover change for every location in the study area is traced, and the specific nature of such change related to human activities can also be identified.

2. Methodology

The generic approach of this study is the temporal trajectory analysis but based on the post-classification comparison method, which is commonly employed in land cover change detection studies (Miller *et al.* 1998, Larsson 2002, Yang and Lo 2002, Zhang *et al* 2002, Narumalani *et al.* 2003, Dewidar 2004, McConnell *et al.* 2004, Tang *et al.* 2005). A unified land cover classification scheme was established for classification of images. The classification images were then used for the analysis of temporal trajectories and the spatial pattern of land cover change in the past 30 years in the study area.

2.1 *Study area and data*

The study area covers about 64 km^2 and is centred at about 41°5′ N and 85°43′ E in Donghetan Township, Yuli County, Xinjiang Uygur Autonomous Region, China. It locates at the middle reach of Tarim River, the longest inland river of China (figure 1). At the fringe of Taklimakan Desert, the 'green corridor' of Tarim Basin is one of the most important habitation areas in the arid zone of China. The landscape in Donghetan is typical of Tarim River Valley, with a generally dry and harsh environment, represented by typical desert vegetation and soils. With increasing land development in recent decades, the fragile environment has experienced quite remarkable change, largely reflecting the general development trend and temporal effects of government policies and administrative measures.

In the past 20 years, the population has increased rapidly and large areas of cropland have been reclaimed. For example, the population in Yuli County, where the study area is located, increased from 29 700 in 1980 to 99 600 in 2000. The cultivated farmland increased more than three-fold, from 6740 ha in 1980 to 21 390 ha in 2000. With the increasing population and cropland reclamation in the upper and middle reaches of Tarim River, water resource consumption increased rapidly. This caused the serious shortage of water resources in the lower reach of the River. As one consequence, the length of the main channel with water flow decreased from 1321 km in the 1960s to 1001 km in 1998.

With the constraints of the availability of remotely sensed data, multi-source imageries were used, including Landsat MSS, TM, ETM and SPOT HRV multi-spectral images. Five multi-temporal remotely sensed images acquired for change detection of this study (table 1). In addition, a multi-spectral 4-m resolution IKONOS image was also acquired in September 2000 to assist in field investigations and accuracy assessment of the image classification. The IKONOS image was geo-referenced to a 1 : 10 000 map using 22 Ground Control Points (GCPs). The other images were then geometrically corrected and registered on the map coordinates using image-to-image registration to the master IKONOS image (table 2). Efforts

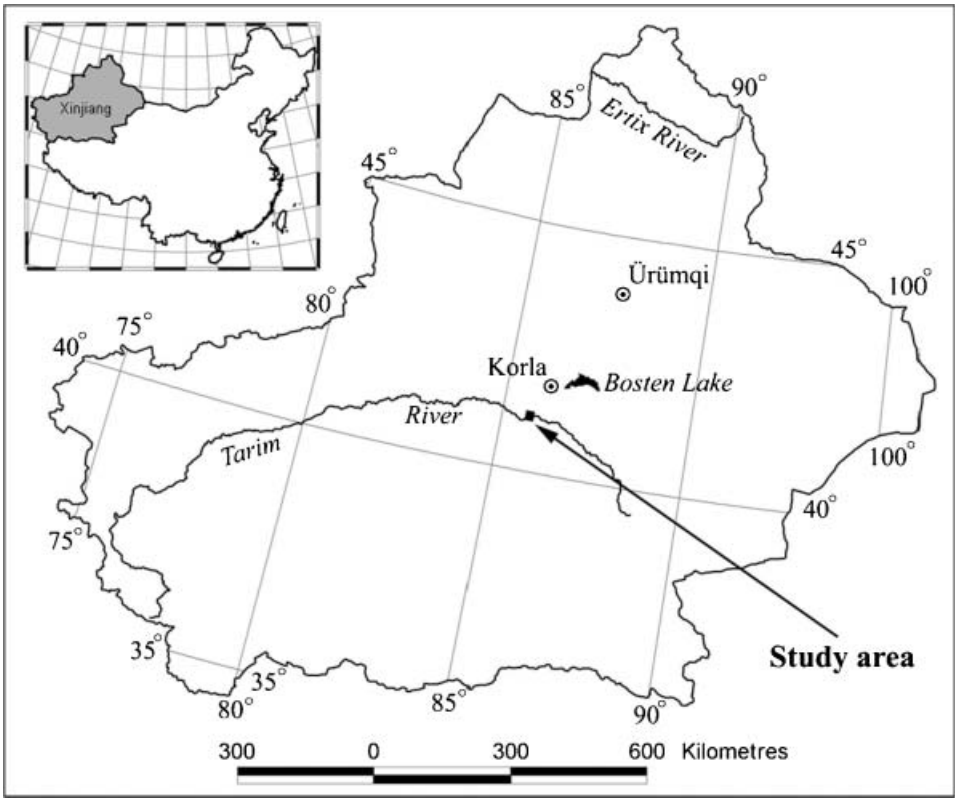

Figure 1. Location map of the study area.

were made to control registration errors to within half a pixel of the image concerned, so that the errors caused by mis-registration would be less critical.

2.2 *Classification*

To minimize seasonal effects of remotely sensed data, the post-classification comparison method was employed for image processing, since this method is less sensitive to radiometric variations between the scenes (Mas 1999). Supervised classification was employed to classify individual images independently, using the maximum likelihood classifier and a unified land cover classification scheme to ensure that the classifications of the multi-scale, multi-temporal images are compatible with each other (table 3). Images were first classified into the Level 2 classes, which were subsequently merged into the five unified classes, as listed in table 3. Training areas were selected based on image interpretation keys established during the field investigation and from interviews with the local inhabitants. A minimum of five training areas containing at least 100 pixels exhibiting uni-modal distribution for DN were selected for each class. The Jeffries–Matusita (JM) separability test (Richards 1995) was then applied to ensure the correctness of the training area selected. For this study, the JM distances between unified classes were kept greater than 1.8 (of the maximum 2.0 as perfectly separable), while the JM distances between Level 2 classes in the same unified class were greater than 1.4. The classification was conducted using PCI Geomatica image processing software.

Table 1. Data used in this research.

Satellite	Sensor	Path/Row	Resolution (m)	Acquisition date
Landsat 1	MSS	154/31	57*	3/7/1973
Landsat 2	MSS	154/31	57*	12/10/1976
SPOT 1	HRV	216/266/9	20	20/7/1986
Landsat 5	TM	143/31	30	25/9/1994
Landsat 7	ETM	143/31	30	17/9/2000

*Resampled resolution.

Table 2. RMS errors on the geometric correction and registration of the images.

	RMSE			
	X (pixels)	*X* (m)	*Y* (pixels)	*Y* (m)
MSS (1973)	0.23	13.11	0.35	19.95
MSS (1976)	0.38	21.66	0.49	27.93
SPOT (1986)	0.21	4.20	0.22	4.40
TM (1994)	0.24	7.20	0.20	6.00
ETM (2000)	0.17	4.85	0.16	4.56

Table 3. Unified land cover classification scheme for multi-scale, multi-temporal images. The numbers denote the land-use class code in individual classifications.

Level 1 classes	Level 2 classes	ETM (2000)	TM (1994)	SPOT (1986)	MSS (1976)	MSS (1973)	Unified classes
Cropland	Cropland	1	1	–	–	–	Cropland (1)
Grass and woodland	Dense grass and woodland	2	2	2	2	2	Grass and woodland (2)
	Sparse grass and woodland	3	3	3	3	3	
	Mowing land	4	–	–	–	–	
	Salty grass	5	5	5	5	5	Salty grass (3)
Water body	Ponds	6	6	6	6	6	Water body (4)
	River	7	7	7			
Unused land	Bare ground and sand dunes	8	8	8	8	8	Bare ground (5)

2.3 *Post-classification sorting*

Classification results were then merged into compatible groups, as shown in table 3. This processing was necessary in order to:

(1) maintain compatibility and comparability between classes in different multi-scale, multi-temporal images,
(2) reduce the number of classes to simplify the analysis of changes in the trajectories of land-use, and
(3) minimize potential errors of classification, since it was already known that some of the classes of land use (e.g., croplands) did not exist in early images. A majority filter is also applied on individual classified images to remove isolated pixels.

2.4 *Accuracy assessment*

In this study we have chosen stratified random sampling scheme for selecting sample points of reference data for classification accuracy assessment. 790 sample points were generated and transferred to GIS. They were then overlaid with the classified images as well as the high-resolution IKONOS multi-spectral image.

Collecting reference data for accuracy assessment on multi-temporal images always presents a serious problem for researchers, because simultaneous 'ground truthing' data over a long period of time are very difficult, if not impossible, to find. In this study, we could only acquire a high-resolution IKONOS multi-spectral image that was simultaneous with the 2000 ETM data. Although the IKONOS image has a high enough resolution for 'ground truthing', the 'time gaps' between this 'reference image' and some historical images are large.

In this study, we directly used the IKONOS image as the source of the reference data to assess the results of the 2000 ETM classifications. For the other four historical images, we used the IKONOS image as the basis for comparison for proper interpretation. By this means, obvious land cover changes such as grasslands to water and bare ground to cropland could be reliably detected by image interpretation. Field visits and interviews were also conducted for sample points where a clear relationship between the present and historical images could not be established.

2.5 *Establishing land cover change trajectory*

Spatio-temporal land cover change patterns have been an active research field (Roy and Tomar 2001, Weng 2001), and the concept and methodology of change trajectory has been developed (Mertens and Lambin 2000, Petit *et al.* 2001, Liu and Zhou, 2004). In this study the term trajectory of land cover change refers to successions of land cover types for a given sample unit over more than two observations (epochs).

To establish land cover change trajectories, all classified images were integrated in GIS using raster format with ARC/INFO GIS software so that pixel-based change trajectories (or 'pixel histories') can be established. Based on the classification scheme as shown in table 3, all possible landuse change trajectories are illustrated in figure 2.

Note that there was no cropland found in this area before the 1990s so that the class 'C' is not included in the classification of the 1973, 1976 and 1986 images. Based on figure 2, a landuse change trajectory can be specified. For example, as highlighted in figure 2, a trajectory can be specified as G→W→G→G→C, meaning that the land was found to be grass/woodland in 1973, water body (flooded) in 1976, grass/woodland again in 1986 and 1994, and cultivated as cropland in 2000.

To analyse temporal human impact on the environment, we have classified all found trajectories into three generic classes, namely, unchanged, human-induced change and natural changes. The *unchanged* class includes trajectories such as G→G→G→G→G and W→W→W→W→W indicating that the same land cover type was found on the sample point over the past 30 years. Some ambiguous cases (e.g. S→S→G→S→S or G→G→G→C→G) are also included in this type considering that possible classification errors may create once-only false classes in the trajectory. The *human-induced* change class includes decisive changes due to human activities such as building dams/reservoirs and cultivation. These changes are

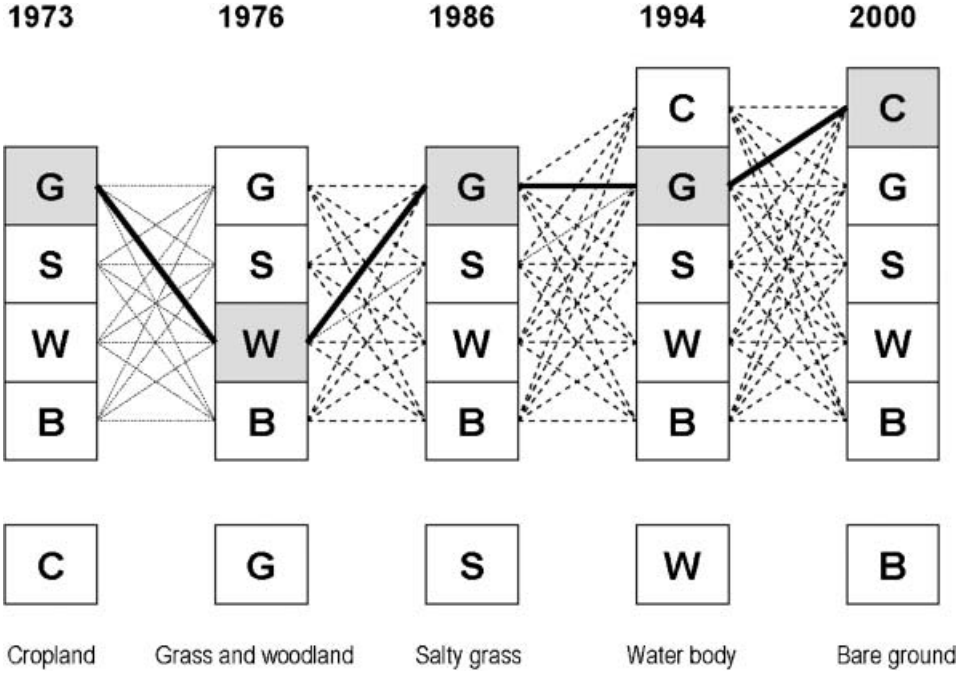

Figure 2. All possible landuse change trajectory identified for the study area. The highlighted land cover change history (presented in thick line) shows a change trajectory as G→W→G→G→C, meaning that the land was found to be grass/woodland in 1973, water body (flooded) in 1976, grass/woodland again in 1986 and 1994, and cultivated as cropland in 2000.

often irreversible so that they represent the major human impact on the environment. The representative trajectories of this class include, e.g., G→G→G→C→C, S→S→G→G→C, and G→G→W→W→W. The *natural* change class includes those indecisive changes due to natural processes or minor human activities such as light grazing. For example, grassland may be flooded during summer and subsequently dried out as salty grass because of strong evapotranspiration. Examples of trajectories of this class are G→W→B→G→G (flooded, eroded and recovered) and G→W→G→W→G (repeatedly flooded). The classification of trajectories is summarized in table 4.

3. Results and discussion

3.1 *Image classification*

The five multi-temporal images were independently classified using the unified land cover classification scheme proposed in this study. It is obvious that higher spectral and/or spatial resolution satellite images have a better ability to separate more classes. However, these level 2 classes need to be merged in post-classification processes so that all multi-platform images can be compared. The classification results are shown in figure 3.

The overall accuracies for image classifications range from 85.8% to 89.8%, with Kappa coefficients ranging from 0.66 to 0.78 (table 5). Generally, the classification on images with higher spatial resolution yields better accuracy results. Although the

Table 4. Classification of landuse change trajectories.

Level 1 classes	Level 2 classes	Description	Trajectory examples
Unchanged	Grass/woodland	No change*	G→G→G→G→G
	Salty grass	No change*	S→S→S→S→S
	Water body	No change*	W→W→W→W→W
	Bare ground	No change*	B→B→B→B→B
Human-induced	Old cultivation	Changed to and remained as cropland since 1994	G→G→G→C→C
	New cultivation	Changed to and remained as cropland since 2000	S→S→G→G→C
	Reservoirs/ponds	Changed to and remained as water bodies since 1986	G→G→W→W→W
Natural	Grass/woodland	Periodical changes between cover G and S	G→S→G→G→S
	Flooded	Periodical changes between cover W and other types	G→W→G→W→G
	Bare ground	Periodical changes between cover B and other types	G→B→B→G→B

*Some ambiguous cases are also included considering that possible classification error may create a once-only false class in the trajectory.

overall accuracies are quite similar for all the classification results, the Kappa coefficients demonstrate much larger ranges. The Kappa of low-resolution MSS classifications were 0.66 and 0.73, in comparison to 0.78–0.83 of those of higher-resolution SPOT, TM and ETM classification.

3.2 *Area statistics*

Table 6 and figure 4 show the area statistics of land cover types and their change over the 30 year study period. According to the local government record, large-scale cultivation started in this area in 1992 and cropped farmland has increased rapidly since then. This change is confirmed by the findings of this study. From the area statistics, it is shown that cropland increased from 4.0% to 12.6% of the total area—three-fold increase in six years. Another significant human impact is the construction of a dam in the north of the study area at the end of 1970s and early 1980s, resulting in flooding of a vast area of grass/woodlands. The grass/woodland area decreased from 72.2% (1976) to 65.2% (1986) during this period, while the water body area increased from 9.6% to 18.0% of the total study area. It is also shown that the area of increasing cropland largely came from salt grass (5.9% (1986)→2.7% (2000)) and water body (18.0% (1986)→8.6% (2000)). This is largely because most of the cultivated lands are located along the river bands of Tarim River in the south and east part of the study area, with the construction of dykes along the river bed to prevent flooding. Cover types with less favourite cultivation conditions (particularly lack of water supply), such as grass/woodland and bare ground, have hardly changed during the 30 year period. The flood effect showed by significant temporary increasing water body and decreasing grass/woodland on the 1994 image should also be noted.

3.3 *Land cover change trajectories*

Table 7 shows that land cover trajectory analysis can display the histories of land cover change over the study period and their nature related to different driving

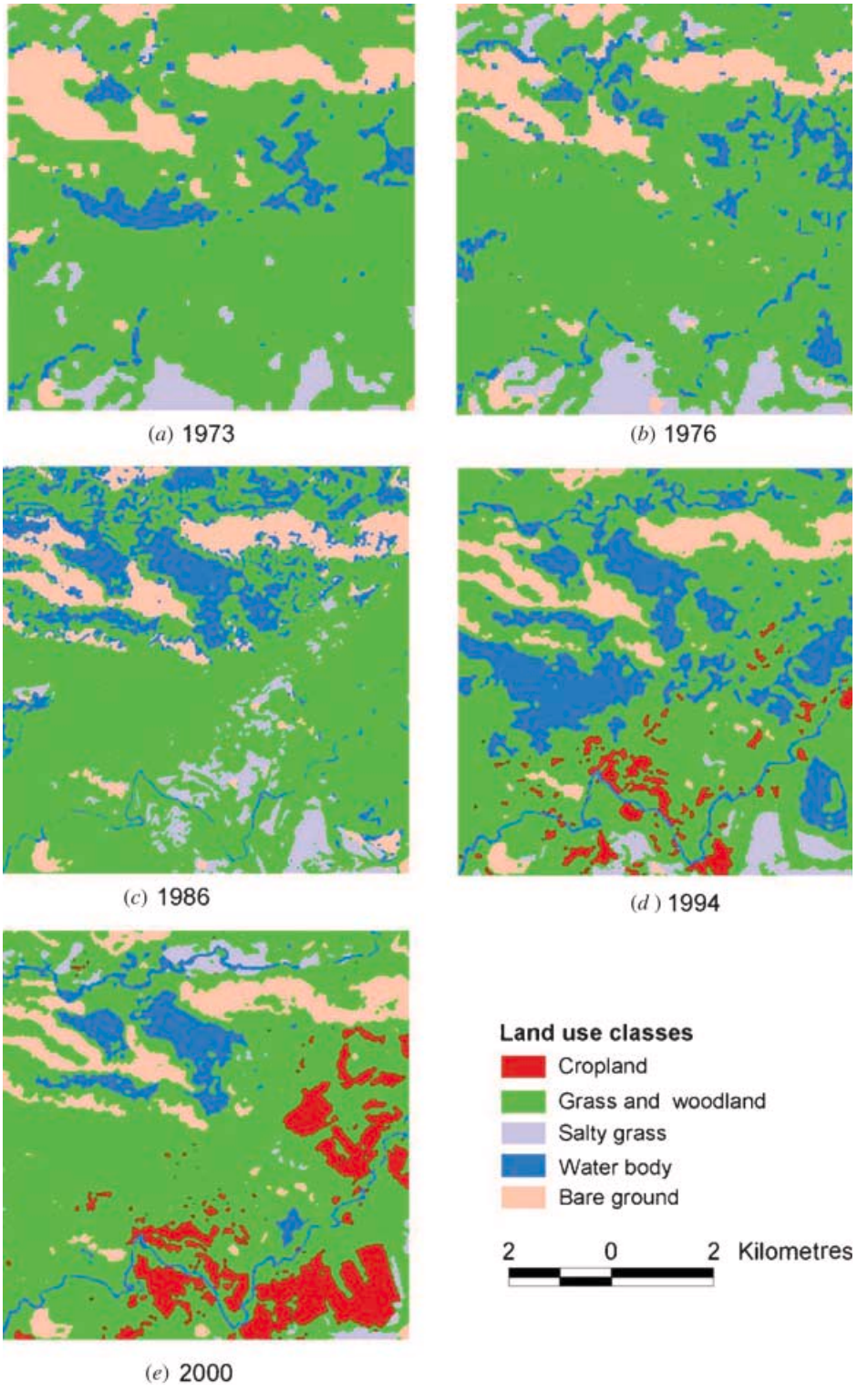

Figure 3. 1973–2000 classified images of land cover types.

Table 5. Overall accuracy assessment.

	MSS (1973)	MSS (1976)	SPOT (1986)	TM (1994)	ETM (2000)
Overall accuracy (%)	88.9	85.8	88.9	89.8	87.1
Kappa	0.73	0.66	0.79	0.83	0.78

Table 6. Area statistics of the land cover types over the 30-year study period.

		1973	1976	1986	1994	2000
Cropland	(ha)	–	–	–	254.3	797.0
	(%)	0	0	0	4.0	12.6
Grass/woodland	(ha)	4746.8	4577.2	4129.9	3811.9	4153.2
	(%)	74.9	72.2	65.2	60.2	65.6
Salty grass	(ha)	331.1	416.4	376.1	202.6	170.7
	(%)	5.2	6.6	5.9	3.2	2.7
Water body	(ha)	476.9	608.8	1143.3	1441.2	547.8
	(%)	7.5	9.6	18.0	22.7	8.6
Bare ground	(ha)	781.3	733.7	686.7	626.1	667.1
	(%)	12.3	11.6	10.8	9.9	10.5

forces of land cover change. During the 30-year study period, the unchanged area occupies 42.8% of the total area, human-induced changes occupied 17.5%, and natural change area occupies 39.7%. For the unchanged area, grass/woodland constitutes 80.3%. For human-induced change, new cultivation occupies 60.8%. For the natural change area, the flooded area obviously dominates, constituting 64.3%. Given the fact that the study area is quite remote and human activities appear to be quite limited, it is understandable that most environmental change is due to natural forces (e.g. flood) rather than human activities. However, it should also be noted that since the early 1990s, human impact starts to play an important role on the environmental change, by altering the natural courses of water and surface materials. Although the total area of human-induced change is still relatively small (<20%), its pace of growth is alarming.

The natural processes relate to natural changes such as flooding and river channel migration. They play a very important role in keeping the sustainability of the natural ecosystem in the study area (e.g. providing the water supply for grassland and woodland). Human activities such as dyke construction (classified here as

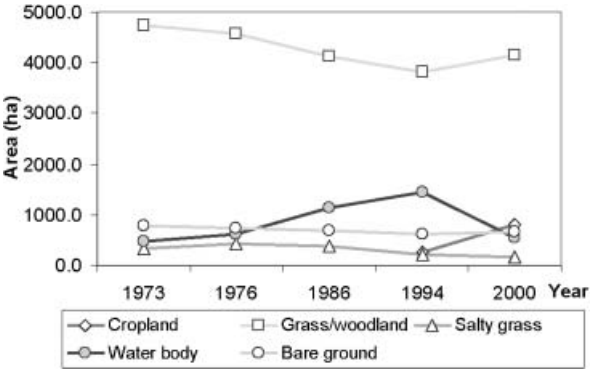

Figure 4. 1973–2000 area change of land cover types.

Table 7. Classification of land-use change trajectories.

Level 1 classes	Level 2 classes	Area (ha)	%
Unchanged	Grass/woodland	2177.5	34.5
	Salty grass	7.7	0.1
	Water body	47.0	0.7
	Bare ground	478.0	7.5
	Sub-total	2710.2	42.8
Human-induced	Old cultivation	124.0	2.0
	New cultivation	675.4	10.7
	Reservoirs/ponds	311.8	4.9
	Sub-total	1111.2	17.5
Natural	Grass/woodland	318.4	5.0
	Flooded	1618.0	25.5
	Bare ground	578.2	9.1
	Sub-total	2514.6	39.7
Total		6336.1	100.0

human-induced changes) will alter the course of natural processes resulting in further deterioration of the natural ecosystem along the Tarim River.

3.4 *Spatial distribution of landuse change trajectories*

Figure 5 shows the spatial distribution of landuse change trajectories in the past 30 years. In the study area, the human-induced changes mainly appeared in two areas, namely, cultivation in south and southeast along the Tarim River, and dam/reservoir construction in the north. In between the two areas, human impact was limited and natural change was predominated by flooding. It should also be noted that areas of natural change with bare ground most likely appeared at the fringe of unchanged bare ground areas, indicating the temporary cover changes in those bare ground areas. Since the total bare ground area had very little change (12.3 (1973)→10.5 (2000), table 6), there is no evidence which shows expansion or shrinking of the bare ground area (mostly sand dunes), nor desertification processes in the study area during the study period.

4. Conclusion

In this paper, we have demonstrated research which studies the spatio-temporal pattern of land cover change in the fragile ecosystem of arid environments of China. Multi-scale and multi-temporal remotely sensed images, including Landsat MSS, TM, ETM and SPOT HRV, were used to analyse the land cover change trajectories and to identify the human-induced environmental change, such as cultivation and dam/reservoir construction. The study shows that using the auto-classification approach an overall accuracy of 85–90% with a Kappa coefficient 0.66–0.78 was achieved for individual image classification. The temporal trajectories of land-use change were established and their spatial distribution analysed. It is shown that natural forces such as flood were still dominating the environmental processes of the study area, with unchanged (42.8% of the total area) and indecisive changes between land cover types (39.7%). However, human-induced changes, constituting 17.5% of the total area, start to play more important role in environmental change. This was demonstrated by the three-fold increase of croplands in the last six years and overall 5% of the area being permanently submerged due to the construction of dam and reservoirs since the 1980s.

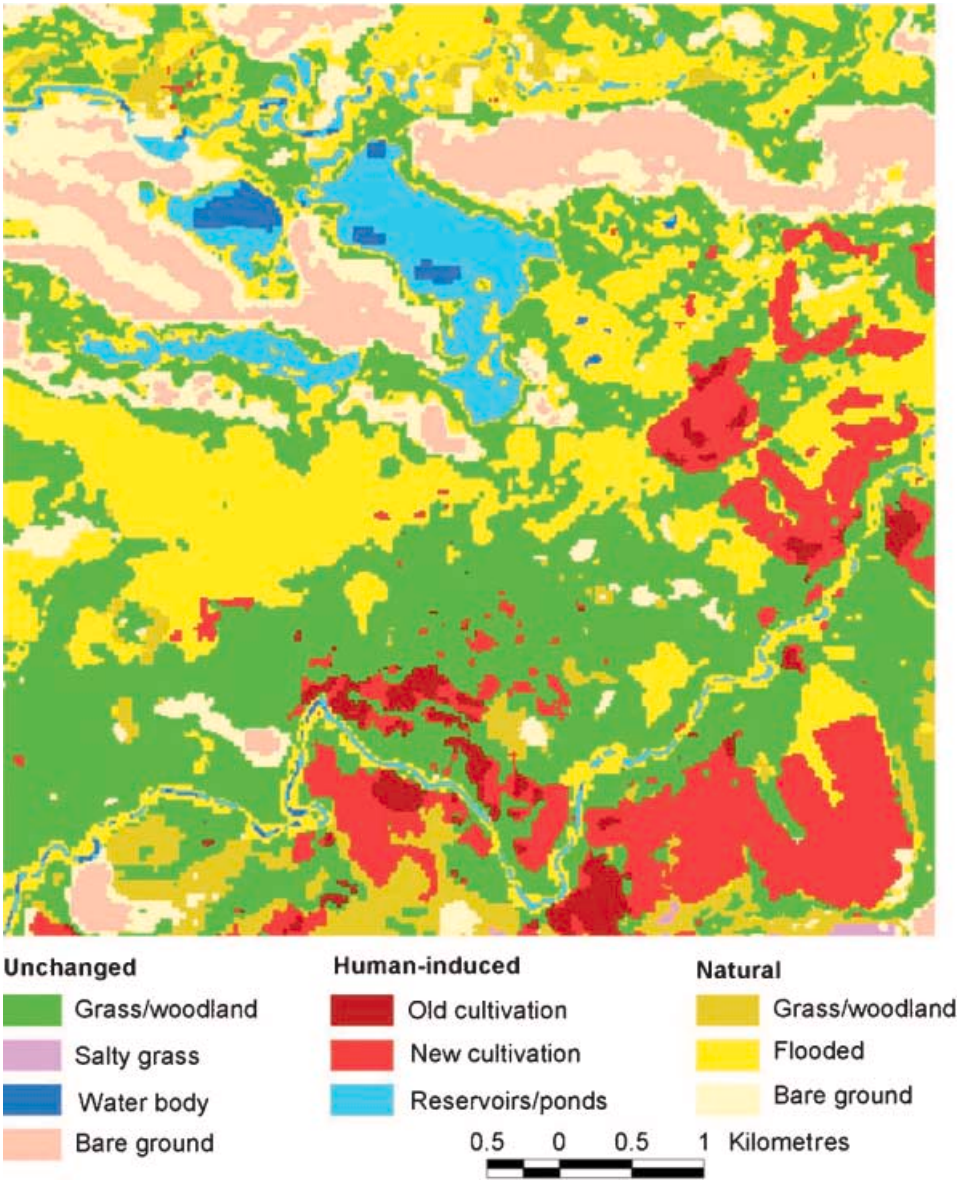

Figure 5. The trajectory classes of land cover change from 1973 to 2000.

This study has demonstrated an efficient and practical approach for analysing environmental changes in an arid environment by integrating multi-temporal and multi-scale remotely sensed data from various sources. In this study, we extended the concepts and methodology of change trajectory analysis to the study of an arid environment. With this approach, human-induced changes, which represent an irreversible impact on the environment, can be extracted from changes caused by natural forces. Regional management can therefore focus on the human-induced changes that have been identified, and on their impact, to achieve the goals of environmentally sound land management practices and sustainable economic development.

Further studies will be focused on the methodology for assessing and modelling the uncertainty of the change trajectory analysis and its impact on environmental change applications. Through further studies on the spatio-temporal patterns and relationships between cover types and local land-use practices, the ultimate goal of this study is to assess human activities and predict environmental responses, particularly the long-term irreversible consequences, so that better, science-based management decisions on land management and development can be made.

Acknowledgements

This research was supported by National Key Basic Research and Development Program (2006CB701304), Research Grants Council Competitive Earmarked Research Grant (HKBU 2026/04P), and Hong Kong Baptist University Faculty Research Grant (FRG/03-04/II-66). The authors would like to thank the staff of Xinjiang Institute of Ecology and Geography, Chinese Academy of Sciences for their support during the fieldwork.

References

COPPIN, P., JONCKHEERE, I., NACKAERTS, K., MUYS, B. and LAMBIN,, 2004, Digital change detection methods in ecosystem monitoring: a review. *International Journal of Remote Sensing*, **25**, pp. 1565–1596.

CREWS-MEYER, K.A., 2001, Assessing landscape change and population-environment interactions via panel analysis. *Geocarto International*, **16**, pp. 69–79.

DESSAY, N., LAURENT, H., MACHADO, L.A.T., SHIMABUKURO, Y.E., BATISTA, G.T. and DIEDHIOU, A., 2004, Comparative study of the 1982–1983 and 1997–1998 El Niño events over different types of vegetation in South America. *International Journal of Remote Sensing*, **25**, pp. 4063–4077.

DEWIDAR, K.H.M., 2004, Detection of land use/land cover changes for the northern part of the Nile delta (Burullus region), Egypt. *International Journal of Remote Sensing*, **25**, pp. 4079–4089.

HARRIS, R., 2003, Remote sensing of agriculture change in Oman. *International Journal of Remote Sensing*, **24**, pp. 4835–4852.

HEROLD, M., GOLDSTEIN, N.C. and CLARKE, K.C., 2003, The spatiotemporal form of urban growth: Measurement, analysis and modelling. *Remote Sensing of Environment*, **86**, pp. 286–302.

HERRMANN, S.M., ANYAMBA, A. and TUCKER, C.J., 2005, Recent trends in vegetation dynamics in the African Sahel and their relationship to climate. *Global Environmental Change*, **5**, pp. 394–404.

HOUHOULIS, P.F. and MICHENER, W.K., 2000, Detecting wetland change: a rule-based approach using NWI and SPOT-XS data. *Photogrammetric Engineering & Remote Sensing*, **66**, pp. 205–211.

KAWABATA, A., ICHII, K. and YAMAGUCHI, Y., 2001, Global monitoring of inter-annual changes in vegetation activities using NDVI and its relationships to temperature and precipitation. *International Journal of Remote Sensing*, **22**, pp. 1377–1382.

LAMBIN, E.F. and EHRLICH, D., 1997, Land-cover changes in sub-Saharan Africa, 1982–1991: application of a change index based on remotely sensed surface temperature and vegetation indices at a continental scale. *Remote Sensing of Environment*, **61**, pp. 181–200.

LARSSON, H., 2002, Analysis of variations in land cover between 1972 and 1990, Kassala Province, Eastern Sudan, using Landsat MSS data. *International Journal of Remote Sensing*, **23**, pp. 325–333.

LIU, H. and ZHOU, Q., 2004, Accuracy analysis of remote sensing change detection by rule-based rationality evaluation with post-classification comparison. *International Journal of Remote Sensing*, **25**, pp. 1037–1050.

LIU, H. and ZHOU, Q., 2005, Establishing a multivariate spatial model for urban growth prediction using multi-temporal images. *Computers, Environment and Urban Systems*, **29**, pp. 580–594.

LIU, X. and LATHROP JR, R.G., 2002, Urban change detection based on an artificial neural network. *International Journal of Remote Sensing*, **23**, pp. 2513–2518.

LIU, Y., NISHIDA, S. and YANO, T., 2004, Analysis of four change detection algorithms in bi-temporal space with a case study. *International Journal of Remote Sensing*, **25**, pp. 2121–2139.

LU, D., MAUSEL, P., BRONDÍZIO, E. and MORAN, E., 2004, Change detection techniques. *International Journal of Remote Sensing*, **24**, pp. 2365–2407.

LUNETTA, R.S., JOHNSON, D.M., LYON, J.G. and CROTWELL, J., 2004, Impacts of imagery temporal frequency on land-cover change detection monitoring. *Remote Sensing of Environment*, **89**, pp. 444–454.

MAKTAV, D. and ERBEK, F.S., 2005, Analysis of urban growth using multi-temporal satellite data in Istanbul, Turkey. *International Journal of Remote Sensing*, **26**, pp. 797–810.

MALDONADO, F.D., DOS SANTOS, J.R. and DE CARVALHO, V.C., 2002, Land use dynamics in the semi-arid region of Brazil (Quixaba, PE): characterization by principal component analysis (PCA). *International Journal of Remote Sensing*, **23**, pp. 5005–5013.

MAS, J.F., 1999, Monitoring land-cover changes: a comparison of change detection techniques. *International Journal of Remote Sensing*, **20**, pp. 139–152.

MASEK, J.G., LINDSAY, F.E. and GOWARD, S.N., 2000, Dynamics of urban growth in the Washington DC metropolitan area, 1973–1996, from Landsat observations. *International Journal of Remote Sensing*, **21**, pp. 3473–3486.

MCCONNELL, W., SWEENEY, S.P. and MULLEY, B., 2004, Physical and social access to land: spatio-temporal patterns of agricultural expansion in Madagascar. *Agriculture, Ecosystems and Environment*, **101**, pp. 171–184.

MERTENS, B. and LAMBIN, E.F., 2000, Land-cover-change trajectories in southern Cameroon. *Annals of the Association of American Geographers*, **90**, pp. 467–494.

MILLER, A.B., BRYANT, E.S. and BIRNIE, R.W., 1998, An analysis of land cover changes in the Northern Forest of New England using multitemporal Landsat MSS data. *International Journal of Remote Sensing*, **19**, pp. 245–265.

MUTTITANON, W. and TRIPATHI, N.K., 2005, Land use/land cover changes in the coastal zone of Ban Don Bay. *International Journal of Remote Sensing*, **26**, pp. 2311–2323.

MYNENI, R.B., KEFLING, C.D., TUCKER, C.J., ASRAR, G. and NEMANI, R.R., 1997, Increased plant growth in the northern high latitudes from 1981 to 1991. *Nature*, **386**, pp. 698–702.

NARUMALANI, S., MISHRA, D.R. and ROTHWELL, R.G., 2004, Change detection and landscape metrics for inferring anthropogenic processes in the greater EFMO area. *Remote Sensing of Environment*, **91**, pp. 478–489.

OLSSON, L., EKLUNDH, L. and ARDÖ, J., 2005, A recent greening of the Sahel—trends,patterns and potential causes. *Journal of Arid Environments*, **63**, pp. 556–566.

PETIT, C.C., SCUDDER, T. and LAMBIN, E., 2001, Quantifying processes of land-cover change by remote sensing: resettlement and rapid land-cover changes in south-eastern Zambia. *International Journal of Remote Sensing*, **22**, pp. 3435–3456.

RICHARDS, J.A., 1995, *Remote Sensing Digital Image Analysis*, 2nd Ed. (Berlin: Springer-Verlag).

ROY, P.S. and TOMAR, S., 2001, Landscape cover dynamics pattern in Meghalaya. *International Journal of Remote Sensing*, **22**, pp. 3813–3825.

SINGH, A., 1989, Digital change detection techniques using remotely-sensed data. *International Journal of Remote Sensing*, **10**, pp. 989–1003.

SOUTHWORTH, J., NAGENDRA, H. and TUCKER, C., 2002, Fragmentation of a landscape: Incorporating landscape metrics into satellite analyses of land-cover change. Landscape Research, **27**, pp. 253–269.

TANG, J., WANG, L. and ZHANG, S., 2005, Investigating landscape pattern and its dynamics in Daqing, China. *International Journal of Remote Sensing*, **26**, pp. 2259–2280.

USTIN, S.L. and XIAO, Q.F., 2001, Mapping successional boreal forests in interior central Alaska. *International Journal of Remote Sensing*, **22**, pp. 1779–1797.

WEBER, C., PETROPOULOU, C. and HIRSCH, J., 2005, Urban development in the Athens metropolitan area using remote sensing data with supervised analysis and GIS. *International Journal of Remote Sensing*, **26**, pp. 785–796.

WENG, Q., 2001, A remote sensing–GIS evaluation of urban expansion and its impact on surface temperature in the Zhujiang Delta, China. *International Journal of Remote Sensing*, **22**, pp. 1999–2014.

YANG, X. and LO, C.P., 2002, Using a time series of satellite imagery to detect land use and land cover changes in the Atlanta, Georgia metropolitan area. *International Journal of Remote Sensing*, **23**, pp. 1775–1798.

ZHANG, Q., WANG, J., PENG, X., GONG, P. and SHI, P., 2002, Urban built-up land change detection with road density and spectral information from multi-temporal Landsat TM data *International Journal of Remote Sensing*, **23**, pp. 3057–3078.

ZHAO, G.X., LIN, G. and WARNER, T., 2004, Using Thematic Mapper data for change detection and sustainable use of cultivated land: a case study in the Yellow River delta, China. *International Journal of Remote Sensing*, **25**, pp. 2509–2522.